

Mesophases of Regularly Branched Copolymers

Galen T. Pickett
Department of Physics and Astronomy
California State University Long Beach
1250 Bellflower Blvd.
Long Beach, CA 90840

ABSTRACT

The phase diagram of A/B block copolymers is determined when the A block is a flexible, linear homopolymer, and the B block has a regularly branched tree structure with G generations. The predictions of a classical-path analysis and a lattice self-consistent mean field calculation are in general agreement. The phase diagram is considerably skewed toward keeping the A blocks inside cylindrical or spherical cores with the branched block forming a corona. There is little, if any, tendency for the branched arms to fold back to facilitate packing.

INTRODUCTION

As the architecture of hyperbranched molecules [1] has come under more and more spectacular control [2, 3, 4, 5], these molecules could well hold the key to the designed self-assembly of interfacial layers with bio-specific adhesion and surface protection [6] as well as a host of other applications. The application of interest here is gaining extra control over the morphology of linear-dendritic block copolymer melts. Ordinary multiblock copolymers are composed of long runs of same-type monomers (blocks) placed on a linear chain. The strong-segregation-limit phase diagram can be strongly affected by the branching of one of the blocks [7, 8, 9]. Roughly speaking, branchings of the B block favor interfacial curvature forcing the B chains to splay outward, relieving some packing constraints. The diagrams can be shifted towards keeping an extreme minority branched species on the exterior of the domains [8, 9], with a consequently severe distortion of the packed domains. An initial attempt to determine the properties of this system [8] employs an Alexander-deGennes ansatz [10, 11], in which all dendrimer free ends are localized on the same surface. In relaxing this requirement, I have turned to the “classical path” approximation [12, 13] and to Scheutjens and Fleer numerical lattice calculations [14]. While the classical path, the Alexander and the lattice calculations all give similarly distorted phase diagrams, the Alexander approximation is found to be particularly unsuited to estimating free energies for branched chains.

CLASSICAL PATH MODEL

The polymers in question have an A block composed of N_A monomers grafted to a dendrimer composed of B monomers and G generations where each of the $2^G - 1$ branched arms is composed of N_B monomers. Thus, the total number of monomers on the chain is $N = N_A + (2^G - 1)N_B$. The thermodynamic incompatibility of the A and B monomers results in the surface tension γ between A and B rich domains. In the lamellar phase, the A blocks stretch a distance H_A from the common AB interface, and the B blocks stretch a distance H_B . Letting

$H = H_A + H_B$ be the overall stripe width, and letting ϕ stand for the overall volume fraction of the B species per chain, with σ copolymers per unit AB interface, the lamellar phase free energy is

$$F_{lam} = \sigma^2 N \left[\frac{\pi^2}{8} (1 - \phi) + \langle f_B(z_o, \phi, G) \rangle \right] + \frac{\gamma}{\sigma}, \quad (1)$$

where $f_B(z_o, \phi, G)$ is the dimensionless free energy of a G -branched chain all of whose free ends are held at the position z_o , and the angled brackets stand for a spatial average over all possible values of z_o . The equilibrium packing at the AB interface is then determined by $\partial F_{lam} / \partial \sigma = 0$. Even though the dendrimer has 2^{G-1} free ends, the classical path approximation ensures that each chain segment with the same *chemical rank* has the same statistics [9, 15]. Thus, the notion that some arms of the dendrimer can fold back towards the AB interface to relieve packing is ruled out.

The challenge is to calculate f_B and its spatial average. Using the fact that single dendrimers arrange themselves in a “filled core” [16] scenario (that is, with their free ends distributed throughout their volume rather than concentrated at their exteriors), it is reasonable to make an ansatz (that will have to be checked *a posteriori*) that free ends exist at each $0 < z_o < H_B$, which ensures that the monomer insertion potential, $P(z)$ is *parabolic*:

$$S[z(n)] = \int_0^{GN} dn f(n) \left[\frac{1}{2a^2} \left| \frac{dz}{dn} \right|^2 + P(z(n)) \right], \quad (2)$$

where $P(z) \equiv a - bz^2/2$, and $S[z(n)]$ is the single-dendrimer free energy to hold the dendrimer with its free ends all located at z_o . The factor $f(n)$ counts the multiplicity of statistically equivalent chain segments at each “chemical index,” n , which runs from $n = 0$ at the tips of the dendrimer up to $n = GN_B$ at the AB junction. For $(G-1)N_B < n < GN_B$, there is a single “root” chain, so $f = 1$. For $(G-2)N_B < n < (G-1)N_B$, there are two equivalent branches, so $f = 2$, and so on. Assuming that thermal fluctuations of $z(n)$ around those which minimize $S[z(n)]$ are forbidden, the minimizing trajectory satisfies:

$$\frac{d}{dn} \left(\frac{f(n) dz}{a^2 dn} \right) = -f(n)bz(n), \quad (3)$$

which reduces to a relatively simple equation as long as n does not correspond to one of the junction points where the chain further branches (for each of these n , $f(n)$ is constant):

$$\frac{1}{a^2} \frac{d^2 z}{dn^2} = -bz. \quad (4)$$

Thus, the minimizing trajectory is piecewise harmonic:

$$z(z_o, n) = z_o(A_1 \cos \omega n + B_1 \sin \omega n) \text{ when } 0 < n \leq N_B \quad (5)$$

$$z(z_o, n) = z_o(A_2 \cos \omega n + B_2 \sin \omega n) \text{ when } N_B < n \leq 2N_B, \quad (6)$$

and so on, so that $z(n)$ is determined by $2G$ constants, A_g and B_g . These constants can be determined by demanding that the trajectory is continuous (G conditions), and that the equation of motion, Eq. 3 is satisfied when $f(n)$ changes discontinuously (a further G conditions). Finally, the unknown frequency, ω , (related to the parameter b in the pressure ansatz) must be chosen so that

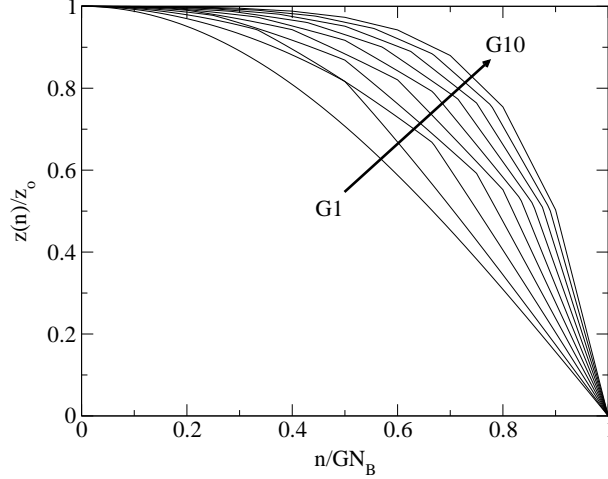


Figure 1: Trajectories, $z(n)/z_0$ for up to G10 dendrimers. The kinks in the trajectory are required for the balance of tensions at those locations where the number of equivalent chain segments decrease by half.

for *each* n the trajectory satisfies $0 < z(n)$ for all except the final monomer for which $z(GN) = 0$. This uniquely specifies the trajectory of the chain, as well as its self-consistent pressure field, so that f_B can be calculated. Figure 1 shows the trajectories for $G = 1 - 10$ thus determined.

With the piecewise harmonic trajectories thus determined, it is possible to determine the distribution of chain free ends, $\xi(z)$ throughout the branched layer:

$$\sigma = \int_z^{H_B} dz_0 \xi(z_0) \frac{dn}{dz}. \quad (7)$$

Thus, chains can be added from the outside of the layer inwards to uniquely fill all available space with b monomers. If this can be done so that the density of ends $\xi(z) > 0$, then a physically relevant solution has been found, and then

$$\sigma^2 N \langle f_B \rangle = \int_0^{H_B} dz_0 S[z(n)] \xi(z_0). \quad (8)$$

The determination of both ξ and f_B must be carried out numerically, but when accomplished results in an estimate of the lamellar phase free energy. The cylindrical and spherical phase free energy can be calculated with the *same* f_B , but the appropriate phase space factor enters into the calculation of ξ and the spatial averages:

$$(H_A + r)^{d-1} \sigma = \int_r^{H_B} dr_0 \xi(r_0) (H_A + r_0)^{d-1} \frac{dn}{dz} \quad (9)$$

where $d = 2$ for cylinders and $d = 3$ for spheres. In both the cylindrical and spherical cases, however, it is necessary to explicitly check that ξ is non-negative.

RESULTS

In Figure 2 we have the phase diagram, in the strongly segregated regime, of these flexible-hyperbranched copolymers. The classical path calculations have been executed for

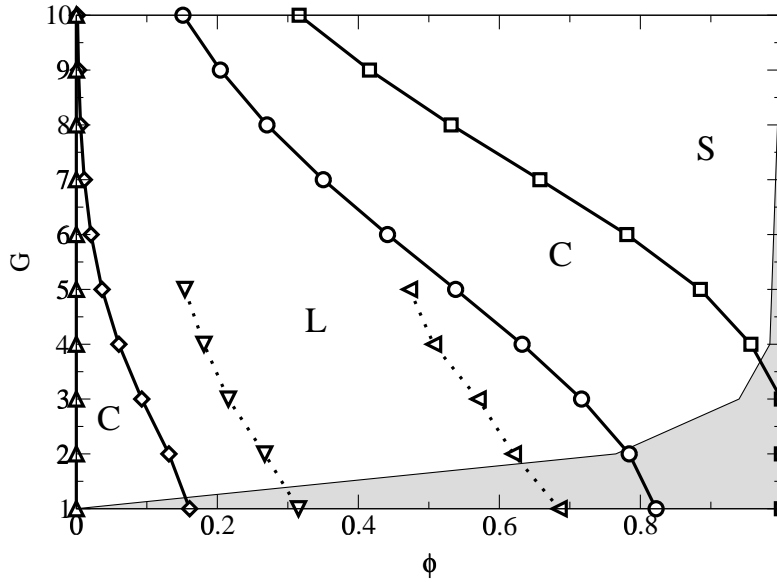


Figure 2: Phase diagram for flexible/dendrimer block copolymers. For large G , the dendrimer component is more and more strongly driven to the outside of the curved domains, and the lamellar phase stability is thus driven towards small ϕ , very asymmetric, compositions. The shaded region represents cases where an unphysical $\xi < 0$ occurs, and the dashed lines represent the results of a numerical lattice calculation on the lamellar-cylindrical phase boundaries.

G1-10, and the lamellar (L), cylindrical (C) and spherical (S) phases have been compared. The solid lines indicate phase boundaries as calculated with the classical path. The lamellar phase is dramatically shifted towards low ϕ (that is, even a small amount of B on the chain is enough to stabilize the lamellar phase). The most dramatic shift occurs for the lamellar-cylinder transition in which the dendrimer occupies the interior of the cylindrical domains (the \diamond symbols in Figure 2). Interestingly, the *spherical phases* are pushed entirely off the phase diagram and either stay there (dendrimer interior to the spherical domains), or enter the phase diagram only at relatively high generation number ($G4$). This hardly matches the known strongly segregated behavior of the G1 copolymers (ordinary diblock copolymers), and is a symptom of the presence of “dead” zones in the calculations for $G < 4$ and of the spherical unit cell approximation that has been used to calculate the classical path free energy.

The boundaries at low ϕ have the dendritic arms inside the cylindrical domains, and the flexible A blocks are on the exterior of the domains. The exterior A blocks *must exhibit* dead zones [12, 17]. In all cases, I have assumed that these A blocks, when confined to the exterior of the domains, are modeled satisfactorily by the Alexander-deGennes picture. For linear chains, this introduces a free energy cost that is larger by a factor of approximately 1.2 than necessary (for flat domains) and is much more satisfactory than the huge overestimate made at higher values of G .

The shaded region in Figure 2 indicates those regions in which the density of ends, $\xi(z_o)$ becomes negative. This signals a breakdown in the parabolic ansatz for the monomer insertion potential. A new self-consistent potential can be calculated, and a reliable estimate for the classical-path with dead-zone free energy can be made, but this goes past the scope of the present development [17].

In Figure 3 I compare the free energies of the branched blocks, f_B , as estimated in the

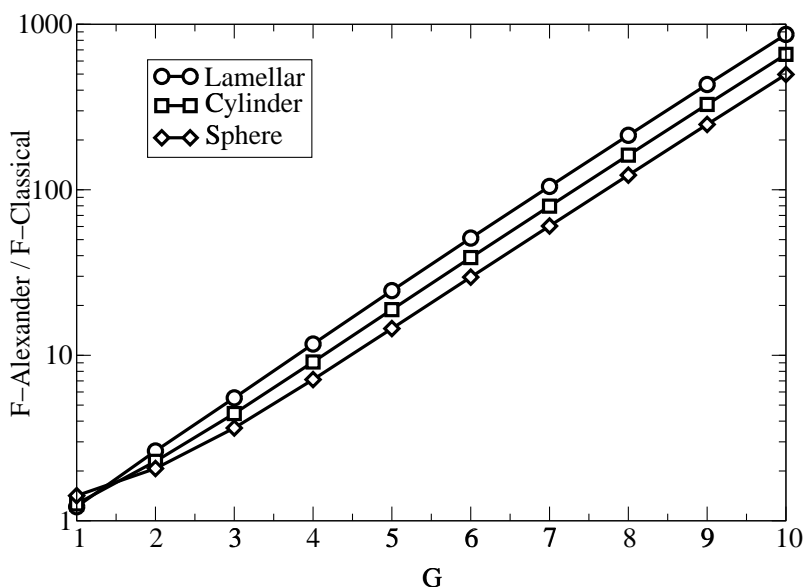


Figure 3: The Alexander-deGennes approximation badly overestimates the free energy of the branched species in these copolymers.

Alexander-deGennes model [8] compared to that determined in the classical path model. As G increases, the Alexander estimate is clearly in serious error, yet the phase diagram as calculated in this model is quite similar to that I have produce in Figure 2. Essentially, the classical path model allows most of the elastic stretching energy to be concentrated *near the AB interface*, so that the dendrimers are essentially unstretched exactly where they have a geometrically large (2^{G-1}) number of equivalent chain segments.

The spherical/cylindrical unit cell approximation can be addressed with the lattice SCF model. Here, the calculations have been executed in two spatial dimensions, so that lamellae and cylinders can be faithfully represented. Spherical domains require a full calculation in three dimensions, at present too expensive for a site-by-site calculation on a three dimensional simple cubic lattice, although such calculations have met success in a dual space of orthogonal functions of the required symmetry [18]. In any case, the dashed lines show the calculated phase boundaries between lamellar and hexagonally-packed cylindrical domains for a variety of dendrimer-flexible copolymers. For all of these calculations, $\chi = 0.5$, and the number of B monomers on the chain has been set to 64. The number of A monomers has been adjusted to attain a desired value of ϕ , ranging from 32 to 128, so that χN varies from a low of 24 up to a maximum of 96. In all cases, these values lie in the strongly segregated regime.

The lamellar phase is drawn away from the extremes of the circular/spherical unit domain approximation, but still tilt severely off toward small ϕ .

CONCLUSION

The flexible-dendrimer copolymer phase diagram has been calculated in the classical path approximation, and compares favorably to a numerical calculation with the lattice SCF theory. While the Alexander-deGennes picture of these copolymer domains also gives a qualitatively

correct phase diagram, that model seriously overestimates the stretching energy of the dendrimer molecules. As previously predicted, the hyperbranching of one of the species is sufficient to dramatically swing the microphase diagram towards low values of branched volume fraction.

References

- [1] Voegtle, F.; Gestermann, S.; Hesse, R.; Schwierz, H.; Windisch, B. *Progress in Polymer Science* **2000** 25 987.
- [2] Ariga, K.; Urakawa, T.; Michiue A.; Sasaki, Y.; Kikuchi, J-I. *Langmuir* **2000** 16 9147.
- [3] Maraval, V.; Laurent, R.; Donnadiou, B.; Mauzac, M.; Caminade, A.-M.; Majoral, J.-P. *J. Am. Chem. Soc.* **2000** 122 2499.
- [4] Pan, Y.; Ford, W. T. *Macromolecules* **1999** 32 5468.
- [5] Watkins, D. M.; Sayed-Sweet, Y.; Klimash, J. W.; Turro, N. J.; Tomalia, D. A. *Langmuir* **1997** 13 3136.
- [6] Irvine, D. J.; Mayes, A. M.; Griffith-Cima, L. *Macromolecules* **1996** 29 6037.
- [7] Milner, S. T. *Macromolecules* **1994** 27 2333.
- [8] Frischknecht, A.; Fredrickson, G. H. *Macromolecules* **1999** 32 6831.
- [9] Galen T. Pickett *Macromolecules In Press*, 1/02.
- [10] Alexander, S. *J. Phys. (Paris)* **1977** 38 983.
- [11] deGennes P.-G. *J. Phys. (Paris)* **1976**, 36 1443.
- [12] Semenov, A. N. *Sov. Phys. JTEP* **1985** 61 733.
- [13] Milner, S. T.; Witten, T. A.; Cates, M. E. *Macromolecules* **1988** 21 2610.
- [14] Fleer, G.; Cohen-Stuart, M. A.; Scheutjens, J. M. H. M.; Cosgrove, T. Vincent, B. *Polymers at Interfaces*; Chapman and Hall: London, 1993.
- [15] Galen T. Pickett, *Macromolecules* **34** 8784 (2001).
- [16] Lescanec, R. L.; Muthukumar, M. *Macromolecules* **1990** 23 2280.
- [17] Ball, R.C.; Marko, J.F.; Milner, S.T.; Witten, T.A. *Macromolecules* **1991** 24 693.
- [18] Matsen, M.W. ; Bates, F.S. *Macromolecules* **1996** 29 1091.